



行政院國家科學委員會補助專題研究計畫成果報告

以費米子-自旋理論探討電荷序和

自旋序條紋相的物理性質

**The study of physical properties of charge-order and  
spin-order stripe phase by using Fermion -spin theory**

90/0128

計畫類別： 個別型計畫

計畫編號： NSC 90-2112-M-032-013

執行期間： 90年8月1日至91年7月31日

計畫主持人： 陳惟堯

處理方式： 可立即對外提供參考

執行單位： 淡江大學物理系

中華民國

91年 10月 21日

# 以費米子-自旋理論探討電荷序和

## 自旋序條紋相的物理性質

The study of physical properties of charge-order and spin-order stripe phase by using Fermion-spin theory

計畫類別： 個別型計畫

計畫編號： NSC 90-2112-M-032-013

執行期間： 90年8月1日至91年7月31日

計畫主持人： 陳惟堯

### 一、中文摘要：

關鍵詞：電子與自旋分離、非費米液體、費米子自旋理論、條紋相

研究氧化物超導材料的最大困難在於如何處理強關聯效應。因為氧化物超導材料是一種典型的強關聯多電子系統，同時又是一種高度各向異性的材料，支配其物理特性的主要是在這些材料中共有的二氧化銅平面裏電子的強關聯效應。強關聯多電子系統的典型特徵是在這類系統中存在一個電子局域單佔據約束條件  $\sum_{\sigma} c_{i\sigma}^{\dagger} c_{i\sigma} \leq 1$ 。如此約束條件處理不好，將導致許多無物理意義的結果。為了處理好這個局域單佔據約束條件，我們採用描述強關聯多電

子系統的一個新的理論方法：

*Fermion-spin* 理論，由馮世平系主任及其合作者在1994年所提出較好處理此類約束條件的強關聯效應理論

[*Phys. Rev. B* 49, 2368 (1994)];

[*Mod. Phys. Lett. B* 7, 1013 (1993)]。在

*Fermion-spin* 理論中已將電子算符寫成費米子  $h_i$  (*holon*) 和 *Hard-core* 玻色子  $S_i$  (*spinon*) 的乘積型式

$C_{i\uparrow} = h_i^{\dagger} S_i^{-}$ ,  $C_{i\downarrow} = h_i^{\dagger} S_i^{+}$ ，然後我們

又證明了此 *Hard-core* 玻色子

$S_i^{-}$  ( $S_i^{+}$ ) 正是一層自旋算符

(*pseudospin operator*), 它的基本性質是在同一格點上服從費米統計, 而在不同格點上遵從玻色統計。

在此一理論框架下, 即使為平均場近似下, 電子的局域單佔據約束條件也可滿足。由於電子的局域單佔據

約束條件已自動滿足, 這也等價於處理好這類系統中的強相關聯效應。我們將利用此 *Fermion-spin* 理論, 探討 *charge-order* 和 *spin-order* 條紋相的物理性質。

## 二、英文摘要 Abstract

Keywords: charge-spin separation, non-Fermi Liquid, Fermion-spin theory, stripe phase

Cuprate superconductors are typical strongly correlated systems, and the physical properties of these materials are mainly determined by the strong electron correlation in copper oxide planes. The strong electron correlation restricts the systems in the no doubly occupied Hilbert subspace, i.e., where there is the single occupancy local constraint  $\sum_{\sigma} C_{i\sigma}^{\dagger} C_{i\sigma} \leq 1$ , which lead to that cuprate superconducting materials are one of the most complicated systems in condensed matter physics so far. If this constraint is not treated properly, many nonphysical meaning result will be obtained.

It is believed that the physics of cuprate superconducting materials may be effectively described by the t-J model or the similar t-t'-J model acting on the space with no doubly occupied sites. Chairman Shiping Feng from Beijing Normal University and his coauthors, proposed a very nice theory for the strong correlation effect to deal with this constraint, namely, the Fermion-spin theory [*Phys. Rev. B* 49, 2368 (1994)]; [*Mod. Phys. Lett. B* 7, 1013 (1993)], under the framework of this theory, a number of abnormal physical properties of these oxide superconductors have been discussed such as charge and spin dynamics. In this research project, we will utilize the Fermion-spin theory to study the properties of the charge-order and spin-order stripe phase.

### 三、緣由與目的

本研究計畫，將研究氧化物高溫超導材料的電荷序 (*charge-order*)，和自旋序 (*spin-order*) 條紋相的物理性質。氧化物超導材料是一種典型的強關聯多電子系統，同時又是一種高度各向異性的材料，支配其物理特性的主要是在這些材料中共有的二氧化銅平面裏電子的強關聯效應。強關聯多電子系統的典型特徵是在這類系統中存在一個電子局域單佔據約束條件

$\sum_{\sigma} c_{i\sigma}^{\dagger} c_{i\sigma} \leq 1$ 。如此約束條件處理不好，將導致許多無物理意義的結果。為了處理好這個困難本研究計畫係應用馮世平系主任及其合作者所提出的 *Fermion-spin* 理論來深入討論氧化物高溫超導才瞭的電荷序電荷序 (*charge-order*)，和自旋序 (*spin-order*) 條紋相的物理性質。

### 四、計畫結果、討論、與自評

我們主要的研究工作是研究強關聯系統與氧化物超導材料反常物理性質，這些研究工作的主要內容如下：

研究工作策重於針對強關聯氧化物材料 *La-Sr-Cu-O* 的 commensurate-incommensurate 轉變的反常磁學性質，亦即通常的理論認為此一轉變涉及條紋相問題，以採用 *t-J* 模型和費米子自旋理論 (*Fermion-spin theory*) 作一系統的研究，並且進一步說明，在沒有摻雜的半滿情況下，*La-Sr-Cu-O* 材料的自旋漲落是 commensurate，這裏散射峰是在布里淵區的  $(\pi, \pi)$  點。隨著摻雜而偏離半滿時，

立即發生 commensurate-incommensurate 轉變，這時 *La-Sr-Cu-O* 材料的磁散射是 incommensurate，並且散射峰是在布里淵區的  $[\pi, (1 \pm \delta)\pi]$  和  $[(1 \pm \delta)\pi, \pi]$  四個點上，這裏  $\delta$  是 incommensurability，在低摻雜時  $\delta$  的數值是隨摻雜濃度的增加而增加，而在高摻雜時， $\delta$  的數值趨於飽和。更特別的是 incommensurate 散射峰的位置與能量無關，但是強度隨能量的增加而減小，最後在高能量時消失，與實驗結果相符。我們在採用 *t-J* 模型和費米子自旋理論 (*Fermion-spin theory*) 下，研究工作進行非常順利，已發表論文共二篇。

### 五、參考文獻

1. Jihong Qin, Yun Song, Shiping Feng, and Wei Yeu Chen, Optical and transport properties in doped two-leg ladder antiferromagnet, *Phys. Rev. B* 65, 155117 (2002).

2. Feng Yuan, Shiping Feng, and Wei Yeu Chen, Incommensurate magnetic fluctuations in the underdoped copper oxide materials, *Commun. Theor. Phys.* 36, 370 (2001).
3. See, e.g., Proceedings of Los Alamos Symposium, edited by K. S. Bedell et al. (Addison -Wesley, California, 1990).
4. E. Dagotto, *Rev. Mod. Phys.* 66, 763 (1994).
5. A. P. Kampf, *Phys. Rep.* 249,219 (1994); M. A. Kasmer et al., *Rev. Mod. Phys.* 70, 897 (1998).
6. T. M. Rice, *Physica C* 282-287, xix (1997), and references therein.
7. P. W. Anderson, *Theory of superconductivity in the high-Tc cooperates* (Princeton, New Jersey, 1997).
8. Shiping Feng, Z. B. Su, and L. Yu, *Phys. Rev. B* 49, 2368 (1994); *Mod. Phys. Lett. B* 7, 1013 (1993).

## Optical and transport properties in a doped two-leg ladder antiferromagnet

Jihong Qin and Yun Song

*Department of Physics, Beijing Normal University, Beijing 100875, China*

Shiping Feng

*Department of Physics, Beijing Normal University, Beijing 100875, China;**The Key Laboratory of Beam Technology and Material Modification of Ministry of Education, Beijing Normal University, Beijing 100875, China;**and National Laboratory of Superconductivity, Academia Sinica, Beijing 100080, China*

Wei Yeu Chen

*Department of Physics, Tamkang University, Tamsui 25137, Taiwan*

(Received 26 September 2001; revised manuscript received 3 December 2001; published 5 April 2002)

Within the  $t$ - $J$  model, the optical and transport properties of the doped two-leg ladder antiferromagnet are studied based on the fermion-spin theory. It is shown that the optical and transport properties of the doped two-leg ladder antiferromagnet are mainly governed by holon scattering. The low-energy peak in the optical conductivity is located at a finite energy, while the resistivity exhibits a crossover from the high-temperature metalliclike behavior to the low-temperature insulatinglike behavior, which is consistent with the experiments.

DOI: 10.1103/PhysRevB.65.155117

PACS number(s): 71.27.+a, 74.20.Mn, 72.10.-d

The undoped cuprate superconductors are typical Mott insulators with the antiferromagnetic long-range order (AFLRO).<sup>1</sup> A small amount of carrier doping to this Mott insulating state drives the metal-insulator transition and directly results in a superconducting transition at low temperatures for low carrier dopings. In the underdoped and optimally doped regimes, the normal state above the superconducting transition temperature shows many unusual properties in the sense that they do not fit in the conventional Fermi-liquid theory, and these unusual normal-state properties of the cuprate superconductors are closely related to the special microscopic conditions, i.e., Cu ions situated in a *square-planar* arrangement and bridged by oxygen ions, weak coupling between neighboring layers, and doping in such a way that the Fermi level lies near the middle of the Cu-O  $\sigma^*$  bond.<sup>1,2</sup> One common feature of these cuprate compounds is the square-planar Cu arrangement.<sup>1,2</sup> It is believed that the two-dimensional anisotropy is prominent in cuprate superconductors due to the layered perovskite structure, and strong quantum fluctuations with the suppression of AFLRO are key aspects.<sup>1,2</sup> However, it has been reported recently that some copper oxide materials, such as  $\text{Sr}_{14}\text{Cu}_{24}\text{O}_{41}$ , do not contain  $\text{CuO}_2$  planes common to cuprate superconductors but consist of two-leg  $\text{Cu}_2\text{O}_3$  ladders and edge-sharing  $\text{CuO}_2$  chains.<sup>3,4</sup> Moreover, the isovalent substitution of Ca for Sr increases the hole density on the ladders by a transfer of preexisting holes in the charge reservoir layers composed of  $\text{CuO}_2$  chains, and then the two-leg ladder copper oxide material  $\text{Sr}_{14-x}\text{Ca}_x\text{Cu}_{24}\text{O}_{41}$  is a superconductor under pressure.<sup>5</sup> Moreover, the experimental data show that the normal state is far from the standard Fermi-liquid behavior.<sup>4,6</sup> The neutron-scattering and muon-spin-resonance measurements on the compound  $\text{Sr}_{14}\text{Cu}_{24}\text{O}_{41}$  indicate that the system is an antiferromagnet with a short-range spin order,<sup>4,7</sup> while the transport measurements on the material  $\text{Sr}_{14-x}\text{Ca}_x\text{Cu}_{24}\text{O}_{41}$  show that the behavior of the

temperature-dependent resistivity is characterized by a crossover from the high-temperature metalliclike behavior to the low-temperature insulatinglike behavior,<sup>5,6</sup> which may be in common with those of the heavily underdoped cuprate superconducting materials.<sup>1,2,8</sup> Further, it has been shown<sup>5,6</sup> from experiments that the ratio of the interladder to in-ladder resistivities is  $R = \rho_a(T)/\rho_c(T) \sim 10$ . This large magnitude of the resistivity anisotropy reflects that the interladder mean free path is shorter than the interladder distance and the carriers are tightly confined to the ladders, and is also the evidence of incoherent transport in the interladder direction; therefore the common two-leg ladders in the ladder materials clearly dominate the most normal-state properties. These ladder copper oxide materials are also natural extensions of the Cu-O chain compounds towards the  $\text{CuO}_2$  sheet structures. Other two-leg ladder compounds have also been found,<sup>9,4</sup> e.g., experiments suggest the realization of the two-leg ladder spin- $\frac{1}{2}$  antiferromagnet in  $(\text{VO})_2\text{P}_2\text{O}_7$ . On the theoretical side, the two-leg ladder antiferromagnet may, therefore, be regarded as the realization of a unique, coherent resonating valence bond spin liquid, which may play a crucial role in the superconductivity of cuprate superconductors as emphasized by Anderson.<sup>10</sup> Therefore it is very important to investigate the normal-state properties of the doped two-leg ladder system using a systematic approach since it may provide deeper insights into the still not fully understood anomalous normal state of cuprate superconductors.

Many researchers have argued successfully that the  $t$ - $J$  model, acting on the Hilbert space with no doubly occupied site, provides a consistent description of the physical properties of the doped antiferromagnet.<sup>10,11</sup> Within the  $t$ - $J$  model, the normal-state properties of cuprate superconductors have been studied,<sup>2,12,13</sup> and the results show that the unusual normal-state properties of cuprate superconductors are caused by the strong electron correlation. Since the strong electron correlation is common for both cuprate supercon-

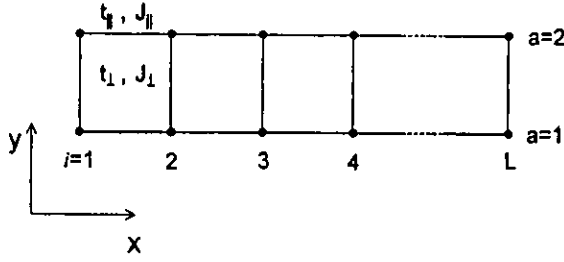


FIG. 1. The  $t$ - $J$  ladder with two legs and  $L$  rungs. The couplings along the legs are  $t_{\parallel}$  and  $J_{\parallel}$ , and those along the rungs  $t_{\perp}$  and  $J_{\perp}$ .

ductors and the doped two-leg ladder antiferromagnet, the unconventional normal-state properties of the doped two-leg ladder antiferromagnet may be similar to those of the cuprate superconductors. In this paper, we study the optical and transport properties of the doped two-leg ladder antiferromagnet within the  $t$ - $J$  model. Our results show that the low-energy peak in the optical conductivity is located at a finite energy ( $\omega \sim 0.2t$ ), while the resistivity exhibits a crossover from the high-temperature metalliclike behavior to the low-temperature insulatinglike behavior.

The basic element of the two-leg ladder materials is the two-leg ladder, which is defined as two parallel chains of ions, with bonds among them such that the interchain coupling is comparable in strength to the couplings along the chains, while the coupling between the two chains that participate in this structure is through rungs.<sup>4</sup> In this case, the  $t$ - $J$  model on the two-leg ladder is expressed as

$$H = -t_{\parallel} \sum_{i\eta a\sigma} C_{i a\sigma}^{\dagger} C_{i+\hat{\eta} a\sigma} - t_{\perp} \sum_{i\sigma} (C_{i1\sigma}^{\dagger} C_{i2\sigma} + \text{H.c.}) - \mu \sum_{i a\sigma} C_{i a\sigma}^{\dagger} C_{i a\sigma} + J_{\parallel} \sum_{i\eta a} S_{i a} \cdot S_{i+\hat{\eta} a} + J_{\perp} \sum_i S_{i1} \cdot S_{i2}, \quad (1)$$

where  $\hat{\eta} = \pm c_0$ ,  $c_0$  is the lattice constant of the two-leg ladder lattice, which is set as unity hereafter,  $i$  runs over all rungs,  $\sigma = (\uparrow, \downarrow)$  and  $a = (1, 2)$  are spin and leg indices, respectively,  $C_{i a\sigma}^{\dagger}$  ( $C_{i a\sigma}$ ) are the electron creation (annihilation) operators,  $S_{i a} = C_{i a\sigma}^{\dagger} \vec{\sigma} C_{i a\sigma} / 2$  are the spin operators with  $\vec{\sigma} = (\sigma_x, \sigma_y, \sigma_z)$  being the Pauli matrices, and  $\mu$  is the chemical potential. This  $t$ - $J$  model is supplemented by the on-site single occupancy local constraint  $\sum_{\sigma} C_{i a\sigma}^{\dagger} C_{i a\sigma} \leq 1$ . The two-leg ladder with  $c$  and  $a$  axes parallel to ladders and rungs, respectively, is sketched in Fig. 1. In the materials of interest, the exchange coupling  $J_{\parallel}$  along the legs is nearly the same as the exchange coupling  $J_{\perp}$  across a rung, and similarly the hopping  $t_{\parallel}$  along the legs is close to the rung hopping strength  $t_{\perp}$ ; therefore, in the following discussions, we will work with the isotropic system  $J_{\perp} = J_{\parallel} = J$ ,  $t_{\perp} = t_{\parallel} = t$ .

In the  $t$ - $J$  model, the strong electron correlation is reflected by the local constraint. To incorporate this local constraint, the fermion-spin theory based on the charge-spin separation,  $C_{i a\sigma} = h_{i a}^{\dagger} S_{i a}^{-}$ ,  $C_{i a\bar{\sigma}} = h_{i a}^{\dagger} S_{i a}^{+}$ , has been proposed,<sup>14</sup> where the spinless fermion operator  $h_{i a}$  keeps

track of the charge (holon), while the pseudospin operator  $S_{i a}$  keeps track of the spin (spinon), and then the local constraint can be treated properly in analytical calculations. Within this fermion-spin representation, the low-energy behavior of the  $t$ - $J$  model (1) can be rewritten as

$$H = t \sum_{i\eta a} h_{i+\hat{\eta} a}^{\dagger} h_{i a} (S_{i a}^{+} S_{i+\hat{\eta} a}^{-} + S_{i a}^{-} S_{i+\hat{\eta} a}^{+}) + t \sum_i (h_{i1}^{\dagger} h_{i2} + h_{i2}^{\dagger} h_{i1}) (S_{i1}^{+} S_{i2}^{-} + S_{i1}^{-} S_{i2}^{+}) + \mu \sum_{i a} h_{i a}^{\dagger} h_{i a} + J_{\parallel \text{eff}} \sum_{i\eta a} S_{i a} \cdot S_{i+\hat{\eta} a} + J_{\perp \text{eff}} \sum_i S_{i1} \cdot S_{i2}, \quad (2)$$

where  $J_{\parallel \text{eff}} = J[(1-\delta)^2 - \phi_{\parallel}^2]$ ,  $J_{\perp \text{eff}} = J[(1-\delta)^2 - \phi_{\perp}^2]$ , the holon particle-hole order parameters  $\phi_{\parallel} = \langle h_{i a}^{\dagger} h_{i+\hat{\eta} a} \rangle$ ,  $\phi_{\perp} = \langle h_{i1}^{\dagger} h_{i2} \rangle$ ,  $\delta$  is the hole doping concentration, and  $S_i^{+}$  and  $S_i^{-}$  are the pseudospin raising and lowering operators, respectively. Since the local constraint has been treated properly in the framework of the fermion-spin theory, the extra gauge degree of freedom related with the electron on-site local constraint under the charge-spin separation does not appear. In this case, the spin fluctuation couples only to spinons, while the charge fluctuation couples only to holons, but the strong correlation between holons and spinons is still considered through the holon's order parameters entering the spinon's propagator and the spinon's order parameters entering the holon's propagator; therefore both holons and spinons contribute to the charge dynamics. In this case, the optical and transport properties of the doped cuprates have been discussed<sup>13</sup> and the results are consistent with the experiments.<sup>12</sup> Following their discussions,<sup>13</sup> the optical conductivity of the doped two-leg ladder antiferromagnet can be expressed as

$$\sigma_c(\omega) = -\frac{\text{Im}\Pi^{(h)}(\omega)}{\omega}, \quad (3)$$

where  $\Pi^{(h)}(\omega)$  is the holon current-current correlation function, which is defined as  $\Pi^{(h)}(\tau - \tau') = -\langle T_{\tau} j^{(h)}(\tau) j^{(h)}(\tau') \rangle$ , where  $\tau$  and  $\tau'$  are the imaginary times and  $T_{\tau}$  is the  $\tau$  order operator. Within the  $t$ - $J$  Hamiltonian (2), the current densities of holons is obtained by the time derivation of the polarization operator using Heisenberg's equation of motion  $j^{(h)} = 2\chi_{\parallel} e t \sum_{ai\eta} \hat{\eta} h_{ai+\hat{\eta}}^{\dagger} h_{ai} + 2\chi_{\perp} e t \sum_i (R_{2i} - R_{1i}) (h_{2i}^{\dagger} h_{1i} - h_{1i}^{\dagger} h_{2i})$ , where  $R_{1i}$  and  $R_{2i}$  are lattice sites of leg 1 and leg 2, respectively, the spinon correlation functions  $\chi_{\parallel} = \langle S_{ai}^{+} S_{ai+\hat{\eta}}^{-} \rangle$ ,  $\chi_{\perp} = \langle S_{1i}^{+} S_{2i}^{-} \rangle$ , and  $e$  is the electronic charge, which is set as unity hereafter. This holon current-current correlation function can be calculated in terms of the holon Green's function  $g(k, \omega)$ . However, in the two-leg ladder system, because there are two coupled  $t$ - $J$  chains, the energy spectrum has two branches. In this case, the one-particle holon Green's function is the matrix, and can be expressed as  $g(i-j, \tau - \tau') = g_L(i-j, \tau - \tau') + \sigma_{xg} \tau(i-j, \tau - \tau')$ , where the longitudinal and transverse parts are defined as  $g_L(i-j, \tau - \tau') = -\langle T_{\tau} h_{ai}(\tau) h_{aj}^{\dagger}(\tau') \rangle$  and  $g_{\tau}(i$

$-j, \tau - \tau') = -\langle T_{\alpha\alpha}(\tau) h_{a'}^{\dagger}(\tau') \rangle$  ( $a \neq a'$ ), respectively. Then after a straightforward calculation,<sup>13</sup> we obtain the optical conductivity of the doped two-leg ladder antiferromagnet as

$$\sigma_c(\omega) = \sigma_c^{(L)}(\omega) + \sigma_c^{(T)}(\omega), \quad (4)$$

with the longitudinal and transverse parts are given by

$$\begin{aligned} \sigma_c^{(L)}(\omega) = & 4t^2 \frac{1}{L} \sum_k (4\chi_{\parallel}^2 \sin^2 k + \chi_{\perp}^2) \int_{-\infty}^{\infty} \frac{d\omega'}{2\pi} A_L^{(h)}(k, \omega') \\ & + \omega) A_L^{(h)}(k, \omega') \frac{n_F(\omega' + \omega) - n_F(\omega')}{\omega}, \end{aligned} \quad (5a)$$

$$\begin{aligned} \sigma_c^{(T)}(\omega) = & 4t^2 \frac{1}{L} \sum_k (4\chi_{\parallel}^2 \sin^2 k - \chi_{\perp}^2) \int_{-\infty}^{\infty} \frac{d\omega'}{2\pi} A_T^{(h)}(k, \omega') \\ & + \omega) A_T^{(h)}(k, \omega') \frac{n_F(\omega' + \omega) - n_F(\omega')}{\omega}. \end{aligned} \quad (5b)$$

respectively, where  $L$  is the number of rungs,  $n_F(\omega)$  is the fermion distribution function. The longitudinal and transverse holon spectral functions  $A_L^{(h)}(k, \omega)$  and  $A_T^{(h)}(k, \omega)$  are obtained as  $A_L^{(h)}(k, \omega) = -2\text{Im}g_L(k, \omega)$  and  $A_T^{(h)}(k, \omega) = -2\text{Im}g_T(k, \omega)$ , respectively, the full holon Green's function  $g^{-1}(k, \omega) = g^{(0)-1}(k, \omega) - \Sigma^{(h)}(k, \omega)$  with the longitudinal and transverse mean-field holon Green's function  $g_L^{(0)}(k, \omega) = 1/2 \sum_{\nu} 1/(\omega - \xi_k^{(\nu)})$  and  $g_T^{(0)}(k, \omega) = 1/2 \sum_{\nu} (-1)^{\nu+1} 1/(\omega - \xi_k^{(\nu)})$ , where  $\nu = 1, 2$ , while the longitudinal and transverse second-order holon self-energy from the spinon pair bubble are obtained by the loop expansion to the second order<sup>13</sup> as

$$\Sigma_L(k, \omega) = \left(\frac{t}{N}\right)^2 \sum_{pq} \sum_{\nu\nu'} \Xi_{\nu\nu'}(k, p, q, \omega), \quad (6)$$

$$\begin{aligned} \Sigma_T(k, \omega) = & \left(\frac{t}{N}\right)^2 \sum_{pq} \sum_{\nu\nu'} \\ & (-1)^{\nu+\nu'+\nu''+1} \Xi_{\nu\nu''}(k, p, q, \omega), \end{aligned} \quad (7)$$

respectively, with  $\Xi_{\nu\nu''}(k, p, q, \omega)$  given by

$$\begin{aligned} \Xi_{\nu\nu''}(k, p, q, \omega) = & \frac{B_{q+p}^{(\nu')} B_q^{(\nu)}}{32\omega_{q+p}^{(\nu')} \omega_q^{(\nu)}} \{2[\gamma_{q+p+k} + \gamma_{q-k}] \\ & + [(-1)^{\nu+\nu''} + (-1)^{\nu'+\nu''}]\}^2 \\ & \times \left( \frac{F_{\nu\nu''}^{(1)}(k, p, q)}{\omega + \omega_{q+p}^{(\nu')} - \omega_q^{(\nu)} - \xi_{p+k}^{(\nu'')}} \right. \\ & + \frac{F_{\nu\nu''}^{(2)}(k, p, q)}{\omega - \omega_{q+p}^{(\nu')} + \omega_q^{(\nu)} - \xi_{p+k}^{(\nu'')}} \\ & \left. + \frac{F_{\nu\nu''}^{(3)}(k, p, q)}{\omega + \omega_{q+p}^{(\nu')} + \omega_q^{(\nu)} - \xi_{p+k}^{(\nu'')}} \right) \end{aligned}$$

$$+ \frac{F_{\nu\nu''}^{(4)}(k, p, q)}{\omega - \omega_{q+p}^{(\nu')} - \omega_q^{(\nu)} - \xi_{p+k}^{(\nu'')}} \Big), \quad (8)$$

where  $\gamma_k = \cos k$ ,  $\lambda = 4J_{\parallel\text{eff}}$ ,  $\epsilon_{\parallel} = 1 + 2t\phi_{\parallel}/J_{\parallel\text{eff}}$ ,  $\epsilon_{\perp} = 1 + 4t\phi_{\perp}/J_{\perp\text{eff}}$ , and

$$B_k^{(\nu)} = B_k - J_{\perp\text{eff}}[\chi_{\perp} + 2\chi_{\perp}^2(-1)^{\nu}][\epsilon_{\perp} + (-1)^{\nu}], \quad (9a)$$

$$B_k = \lambda[(2\epsilon_{\parallel}\chi_{\parallel}^2 + \chi_{\parallel})\gamma_k - (\epsilon_{\parallel}\chi_{\parallel} + 2\chi_{\parallel}^2)], \quad (9b)$$

$$\begin{aligned} F_{\nu\nu''}^{(1)}(k, p, q) = & n_F(\xi_{p+k}^{(\nu'')})[n_B(\omega_q^{(\nu)}) - n_B(\omega_{q+p}^{(\nu)})] \\ & + n_B(\omega_{q+p}^{(\nu)})[1 + n_B(\omega_q^{(\nu)})], \end{aligned} \quad (9c)$$

$$\begin{aligned} F_{\nu\nu''}^{(2)}(k, p, q) = & n_F(\xi_{p+k}^{(\nu'')})[n_B(\omega_{q+p}^{(\nu)}) - n_B(\omega_q^{(\nu)})] + n_B(\omega_q^{(\nu)}) \\ & \times [1 + n_B(\omega_{q+p}^{(\nu)})], \end{aligned} \quad (9d)$$

$$\begin{aligned} F_{\nu\nu''}^{(3)}(k, p, q) = & n_F(\xi_{p+k}^{(\nu'')})[1 + n_B(\omega_{q+p}^{(\nu)}) + n_B(\omega_q^{(\nu)})] \\ & + n_B(\omega_q^{(\nu)})n_B(\omega_{q+p}^{(\nu)}), \end{aligned} \quad (9e)$$

$$\begin{aligned} F_{\nu\nu''}^{(4)}(k, p, q) = & [1 + n_B(\omega_q^{(\nu)})][1 + n_B(\omega_{q+p}^{(\nu)})] - n_F(\xi_{p+k}^{(\nu'')}) \\ & \times [1 + n_B(\omega_{q+p}^{(\nu)}) + n_B(\omega_q^{(\nu)})], \end{aligned} \quad (9f)$$

where  $n_B(\omega_k^{(\nu)})$  is the boson distribution functions, the mean-field (MF) holon excitations  $\xi_k^{(\nu)} = 4t\chi_{\parallel}\gamma_k + \mu + 2\chi_{\perp}t(-1)^{\nu+1}$ , and the MF spinon excitations

$$\begin{aligned} \omega_k^{(\nu)2} = & \alpha\epsilon_{\parallel}\lambda^2 \left[ \frac{1}{2}\chi_{\parallel} + \epsilon_{\parallel}\chi_{\parallel}^2 \right] \gamma_k^2 - \epsilon_{\parallel}\lambda^2 \left[ \frac{1}{2}\alpha \left( \frac{1}{2}\epsilon_{\parallel}\chi_{\parallel} + \chi_{\parallel}^2 \right) \right. \\ & + \alpha \left( C_{\parallel}^z + \frac{1}{2}C_{\parallel} \right) + \frac{1}{4}(1-\alpha) \left. \right] \gamma_k - \frac{1}{2}\alpha\epsilon_{\perp}\lambda J_{\perp\text{eff}}(C_{\perp} \\ & + \epsilon_{\parallel}\chi_{\perp})\gamma_k + \alpha\lambda J_{\perp\text{eff}}(-1)^{\nu+1} \left[ \frac{1}{2}(\epsilon_{\perp}\chi_{\parallel} + \epsilon_{\parallel}\chi_{\perp}) \right. \\ & + \epsilon_{\parallel}\epsilon_{\perp}(\chi_{\perp}^2 + \chi_{\parallel}^2) \left. \right] \gamma_k - \alpha\epsilon_{\parallel}\lambda J_{\perp\text{eff}}(C_{\perp}^z + \chi_{\perp}^2)\gamma_k \\ & + \lambda^2 \left[ \alpha \left( C_{\parallel}^z + \frac{1}{2}\epsilon_{\parallel}^2 C_{\parallel} \right) + \frac{1}{8}(1-\alpha)(1 + \epsilon_{\parallel}^2) \right. \\ & - \frac{1}{2}\alpha\epsilon_{\parallel} \left. \left( \frac{1}{2}\chi_{\parallel} + \epsilon_{\parallel}\chi_{\parallel}^2 \right) \right] + \alpha\lambda J_{\perp\text{eff}}[\epsilon_{\parallel}\epsilon_{\perp}C_{\perp} + 2C_{\perp}^z] \\ & + \frac{1}{4}J_{\perp\text{eff}}^2(\epsilon_{\perp}^2 + 1) - \frac{1}{2}\epsilon_{\perp}J_{\perp\text{eff}}^2(-1)^{\nu+1} - \alpha\lambda J_{\perp\text{eff}} \\ & \times (-1)^{\nu+1} \left[ \frac{1}{2}\epsilon_{\parallel}\epsilon_{\perp}\chi_{\parallel} + \epsilon_{\perp}(\chi_{\parallel}^2 + C_{\perp}^z) + \frac{1}{2}\epsilon_{\parallel}C_{\perp} \right], \end{aligned} \quad (10)$$



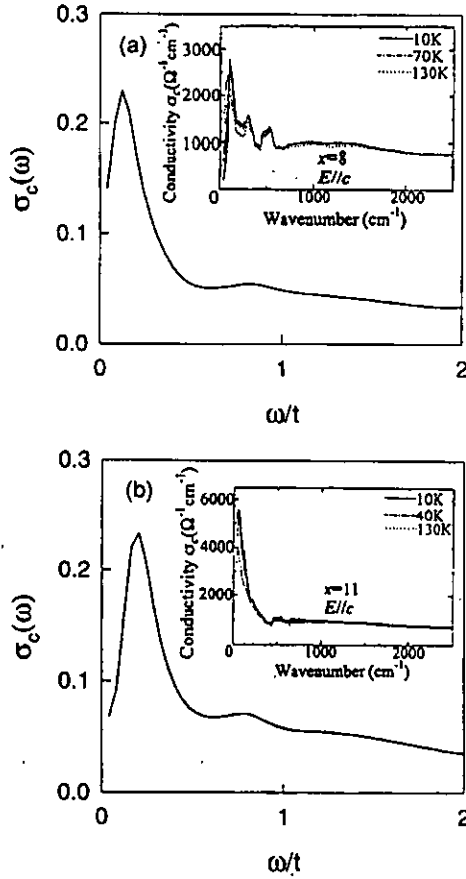


FIG. 2. The optical conductivity of the doped two-leg ladder antiferromagnet at doping (a)  $\delta=0.16$  and (b)  $\delta=0.20$  for parameter  $t/J=2.5$  at temperature  $T=0$ . Inset: the experimental result on  $\text{Sr}_{14-x}\text{Ca}_x\text{Cu}_2\text{O}_{41}$  taken from Ref. 6.

with the spinon correlation functions  $\chi_{\parallel}^z = \langle S_{ai}^z S_{ai+\eta}^z \rangle$ ,  $\chi_{\perp}^z = \langle S_{1i}^z S_{2i}^z \rangle$ ,  $C_{\parallel} = (1/4) \sum_{\eta\eta'} \langle S_{ai+\eta}^+ S_{ai+\eta'}^- \rangle$ , and  $C_{\perp}^z = (1/4) \sum_{\eta\eta'} \langle S_{ai+\eta}^z S_{ai+\eta'}^z \rangle$ ,  $C_{\perp} = (1/2) \sum_{\eta} \langle S_{2i}^+ S_{1i+\eta}^- \rangle$ , and  $C_{\perp}^z = (1/2) \sum_{\eta} \langle S_{1i}^z S_{2i+\eta}^z \rangle$ . In order not to violate the sum rule of the correlation function  $\langle S_{ai}^+ S_{ai}^- \rangle = 1/2$  in the case without AFLRO, the important decoupling parameter  $\alpha$  has been introduced in the mean-field calculation, which can be regarded as the vertex correction.<sup>15</sup> All the above mean-field order parameters have been determined by the self-consistent calculation.<sup>15</sup>

Now we discuss the optical and transport properties of the doped two-leg ladder antiferromagnet. The optical conductivity of the doped Mott insulator, in principle, consists of three different parts: (1) the Drude absorption, (2) absorption across the Mott-Hubbard gap, which rapidly decreases in intensity upon doping, and (3) an absorption continuum within the gap, which reflects the strong coupling between charge carriers and spin excitations. In Fig. 2, we plot the optical conductivity  $\sigma_c(\omega)$  at doping (a)  $\delta=0.16$  and (b)  $\delta=0.20$  for parameter  $t/J=2.5$  at temperature  $T=0$ , in comparison with the corresponding experimental data<sup>6</sup> taken on

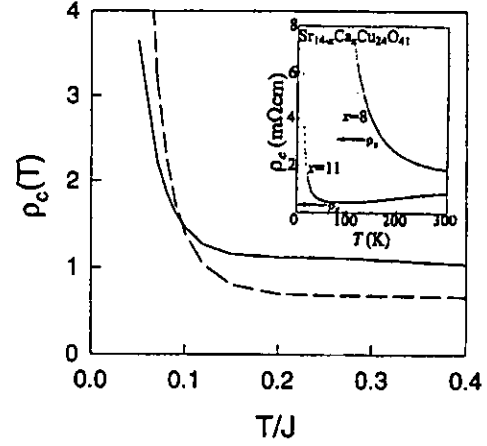


FIG. 3. The resistivity of the doped two-leg ladder antiferromagnet at doping  $\delta=0.16$  (solid line) and  $\delta=0.20$  (dashed line) for parameter  $t/J=2.5$ . Inset: the experimental result on  $\text{Sr}_{14-x}\text{Ca}_x\text{Cu}_2\text{O}_{41}$  taken from Ref. 6.

$\text{Sr}_{14-x}\text{Ca}_x\text{Cu}_2\text{O}_{41}$  (inset), where the hole density on the ladders at  $x=8$  and  $x=11$  is  $\delta=0.16$  and  $\delta=0.20$  per Cu ladder, respectively. From Fig. 2, we find that the optical conductivity consists of two bands separated at  $\omega \sim 0.5t$ : the higher-energy band, corresponding to the midinfrared band, shows a weak peak at  $\omega \sim 0.8t$  unlike a Drude peak, which dominates in the conductivity spectrum of the doped cuprate superconductors, the lower-energy peak in the present ladder systems is located at a finite energy  $\omega \sim 0.2t$ , while the extremely small continuum absorption is consistent with the notion of the charge-spin separation. These behaviors are in agreement with the experimental results of the doped two-leg ladder antiferromagnet.<sup>5,6</sup> In the above calculations, we also find that the optical conductivity  $\sigma_c(\omega)$  of the doped two-leg ladder antiferromagnet is essentially determined by its longitudinal part  $\sigma_c^{(L)}(\omega)$ , this is why in the present ladder systems the midinfrared band is much weaker than the low-energy band, and the conductivity spectrum appears to reflect the one-dimensional nature of the electronic state.<sup>16</sup> This conductivity of the doped two-leg ladder antiferromagnet has been discussed by Kim<sup>17</sup> based on a model of hole pairs forming a strongly correlated liquid, where quantum interference effects are handled using renormalization-group methods, and then the main low-energy features of the experiments are reproduced. Our results in low energy are also consistent with his results.

With the help of the optical conductivity (4), the resistivity can be obtained as  $\rho_c = 1/\lim_{\omega \rightarrow 0} \sigma_c(\omega)$ . The result of  $\rho_c$  at doping  $\delta=0.16$  (solid line) and  $\delta=0.20$  (dashed line) for parameter  $t/J=2.5$  is shown in Fig. 3, in comparison with the corresponding experimental results<sup>6</sup> taken on  $\text{Sr}_{14-x}\text{Ca}_x\text{Cu}_2\text{O}_{41}$  (inset). Our results show that the behavior of the temperature dependence of  $\rho_c(T)$  exhibits a crossover from the high-temperature metalliclike behavior to the low-temperature insulatinglike behavior, but the metalliclike temperature dependence dominates over a wide temperature

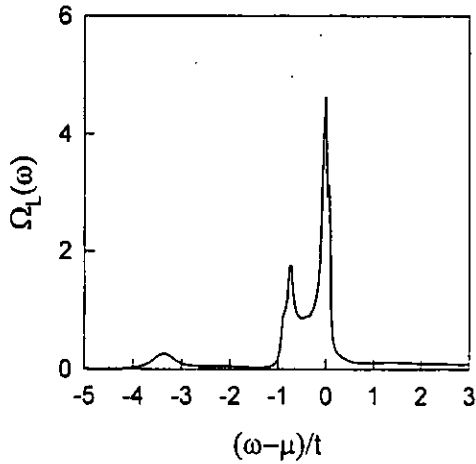


FIG. 4. The holon density of states at doping  $\delta=0.16$  for parameter  $t/J=2.5$  at temperature  $T=0$ .

range, in agreement with the corresponding experimental data.<sup>5,6</sup> The present result also indicates that the behaviors of  $\rho_c(T)$  in the doped two-leg ladder antiferromagnet are very similar to those of the heavily underdoped cuprate superconducting materials<sup>1,2,8</sup> perhaps since both materials have almost same microscopic energy scales and owing to the common corner-sharing  $\text{CuO}_4$  networks.

In the above discussions, the central concern of the optical and transport properties in the doped two-leg ladder antiferromagnet is the quasi-one-dimensionality of the electron state, then the optical and transport properties are mainly determined by the longitudinal charged holon fluctuation. Our present study also indicates that the observed crossovers of  $\rho_c$  for the doped two-leg ladder antiferromagnet seem to be connected with the pseudogap in the charged holon excitations, which can be understood from the physical property of the holon density of states (DOS)  $\Omega_L(\omega) = 1/N \sum_k A_L^{(h)}(k, \omega)$ . This holon DOS has been calculated, and the result at doping  $\delta=0.16$  for parameter  $t/J=2.5$  with temperature  $T=0$  is plotted in Fig. 4. We therefore find that the holon DOS consists of a U-shape pseudogap near the chemical potential  $\mu$ . For a better understanding of the property of this U-shape pseudogap, we plot the phase diagram  $T^* \sim \delta$  at parameter  $t/J=2.5$  in Fig. 5, where  $T^*$  marks the development of the pseudogap in the holon DOS. As seen from Fig. 5, this pseudogap is doping and temperature dependent and grows monotonical as the doping  $\delta$  decreases and disappears at higher doping. Moreover, this pseudogap decreases with increasing temperatures and vanishes at higher temperatures. Since the full holon Green's function (then the holon spectral function and DOS) is obtained by considering the second-order correction due to the spinon pair bubble, the holon pseudogap is closely related to the spinon fluctuation. This holon pseudogap would reduce the holon scattering and thus is responsible for the metallic to insulating crossover in the resistivity  $\rho_c$ . While in the region where the holon pseudogap closes at high temperatures, the charged holon scattering would give rise to the metallic temperature dependence of the resistivity.

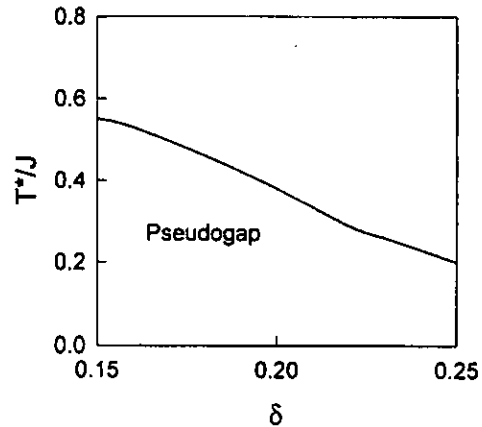


FIG. 5. The normal-state phase diagram  $T^* \sim \delta$  for parameter  $t/J=2.5$ .  $T^*$  marks the development of the holon pseudogap in the holon density of states.

In summary, we have studied the optical and transport properties of the doped two-leg ladder antiferromagnet within the  $t$ - $J$  model. Our result shows that the optical and transport properties of the doped two-leg ladder antiferromagnet are mainly governed by the charged holon scattering. The low-energy peak in the optical conductivity is located at a finite energy, while the resistivity exhibits a crossover from the high-temperature metalliclike behavior to the low-temperature insulatinglike behavior, in agreement with the experiments.

Finally, we emphasize that in the above discussions, only the results of the doped isotropic two-leg ladder system are presented. However, we<sup>18</sup> have also studied the physical properties of the anisotropic system, i.e.,  $J_\perp < J_\parallel$  and  $t_\perp < t_\parallel$ . In this case, the interference effects between the two legs are decreased by decreasing the values of  $J_\perp/J_\parallel$  and  $t_\perp/t_\parallel$ ; this leads to the low-energy peak of the conductivity being located at  $\omega \sim 0$  instead of a finite energy for the isotropic system. On the other hand, it has been shown that the interleg single-electron hopping changes the asymptotic behavior of the interleg spin-spin correlation functions, but their exponents are independent of the interleg coupling strength.<sup>19</sup> We believe that the evolution of the incommensurate magnetic fluctuations with dopings in the doped square lattice antiferromagnet<sup>20</sup> will also occur in the doped two-leg antiferromagnet, and the related theoretical results will be presented elsewhere.

#### ACKNOWLEDGMENTS

The authors would like to thank Dr. Feng Yuan and Xianglin Ke for helpful discussions. This work was supported by the National Natural Science Foundation for Distinguished Young Scholars under Grant No. 10125415, the National Natural Science Foundation under Grants Nos. 10074007 and 90103024, a Grant from the Ministry of Education of China, and the National Science Council under Grant No. NSC 90-2816-M-032-0001-6.

- <sup>1</sup>M.A. Kastner, R.J. Birgeneau, G. Shiran, and Y. Endoh, *Rev. Mod. Phys.* **70**, 897 (1998); A.P. Kampf, *Phys. Rep.* **249**, 219 (1994).
- <sup>2</sup>See, e. g., *Proceedings of Los Alamos Symposium*, edited by K. S. Bedell, D. Coffey, D. E. Meltzer, D. Pines, and J. R. Schrieffer (Addison-Wesley, Redwood City, CA, 1990); P. W. Anderson, *The Theory of Superconductivity in the High- $T_c$  Cuprates* (Princeton University Press, Princeton, NJ, 1997).
- <sup>3</sup>M. Azuma, Z. Hiroi, M. Takano, K. Ishida, and Y. Kitaoka, *Phys. Rev. Lett.* **73**, 3463 (1994).
- <sup>4</sup>E. Dagotto and T.M. Rice, *Science* **271**, 618 (1996), and references therein.
- <sup>5</sup>T. Nagata, M. Uehara, J. Goto, J. Akimitsu, N. Motoyama, H. Eisaki, S. Uchida, H. Takahashi, T. Nakanishi, and N. Mori, *Phys. Rev. Lett.* **81**, 1090 (1998); M. Uehara, T. Nagata, J. Akimitsu, H. Takahashi, N. Mori, and K.K. Kinoshita, *J. Phys. Soc. Jpn.* **65**, 2764 (1996).
- <sup>6</sup>T. Osafune, N. Motoyama, H. Eisaki, S. Uchida, and S. Tajima, *Phys. Rev. Lett.* **82**, 1313 (1999); T. Osafune, N. Motoyama, H. Eisaki, and S. Uchida, *ibid.* **78**, 1980 (1997).
- <sup>7</sup>T. Imai, K.R. Thurber, K.M. Shen, A.W. Hunt, and F.C. Chou, *Phys. Rev. Lett.* **81**, 220 (1998); Y. Sidis, M. Braden, P. Bourges, B. Hennion, S. NishiZaki, Y. Maeno, and Y. Mori, *ibid.* **83**, 3320 (1999).
- <sup>8</sup>H. Takagi, B. Batlogg, H.L. Kao, J. Kwo, R.J. Cava, J.J. Krajewski, and W.F. Peck, *Phys. Rev. Lett.* **69**, 2975 (1992).
- <sup>9</sup>D.C. Johnston, J.W. Johnson, D.P. Goshom, and A.P. Jacobson, *Phys. Rev. B* **35**, 219 (1987).
- <sup>10</sup>P. W. Anderson, in *Frontiers and Borderlines in Many Particle Physics*, edited by R. A. Broglia and J. R. Schrieffer (North-Holland, Amsterdam, 1987), P. 1; *Science* **235**, 1196 (1987).
- <sup>11</sup>F.C. Zhang and T.M. Rice, *Phys. Rev. B* **37**, 3759 (1988); T.M. Rice, *Physica C* **282-287**, xix (1997).
- <sup>12</sup>E. Dagotto, *Rev. Mod. Phys.* **66**, 763 (1994), and references therein.
- <sup>13</sup>Shiping Feng and Zhongbing Huang, *Phys. Lett. A* **232**, 293 (1997); *Phys. Rev. B* **57**, 10 328 (1998).
- <sup>14</sup>Shiping Feng, Z.B. Su, and L. Yu, *Phys. Rev. B* **49**, 2368 (1994); *Mod. Phys. Lett. B* **7**, 1013 (1993).
- <sup>15</sup>J. Kondo and K. Yamaji, *Prog. Theor. Phys.* **47**, 807 (1972); Shiping Feng and Yun Song, *Phys. Rev. B* **55**, 642 (1997).
- <sup>16</sup>P. Horsch and W. Stephan, *Phys. Rev. B* **48**, 10 595 (1993).
- <sup>17</sup>E.H. Kim, *Phys. Rev. Lett.* **86**, 1315 (2001).
- <sup>18</sup>Jihong Qin, Ying Huang, and Shiping Feng (unpublished).
- <sup>19</sup>G.M. Zhang, Shiping Feng, and Lu Yu, *Phys. Rev. B* **49**, 9997 (1994).
- <sup>20</sup>K. Yamada, C.H. Lee, K. Kurahashi, J. Wada, S. Wakimoto, S. Ueki, H. Kimura, Y. Endoh, S. Hosoya, and G. Shirane, *Phys. Rev. B* **57**, 6165 (1998); P. Dai, H.A. Mook, R.D. Hunt, and F. Doğan, *ibid.* **63**, 054525 (2001); Feng Yuan, Shiping Feng, Zhao-Bin Su, and Lu Yu, *ibid.* **64**, 224505 (2001).

## Incommensurate Magnetic Fluctuations in the Underdoped Copper Oxide Materials\*

YUAN Feng,<sup>1,2,3</sup> FENG Shi-Ping<sup>1,2,3</sup> and CHEN Wei-Yeu<sup>4</sup>

<sup>1</sup>Department of Physics, Beijing Normal University, Beijing 100875, China

<sup>2</sup>National Laboratory of Superconductivity, Academia Sinica, Beijing 100080, China

<sup>3</sup>Institute of Theoretical Physics, Academia Sinica, Beijing 100080, China

<sup>4</sup>Department of Physics, Tamkang University, Tamsui 25137, Taiwan

(Received April 28, 2001)

**Abstract** *The doping dependence of magnetic fluctuations in the underdoped copper oxide materials are studied within the  $t$ - $J$  model. It is shown that away from the half-filling, the magnetic Bragg peaks from the dynamical spin structure factor spectrum  $S(k, \omega)$  are incommensurate with the lattice. Although the incommensurability  $\delta(x)$  is almost energy-independent, the dynamical spin susceptibility  $\chi''(k, \omega)$  at the incommensurate wave vectors is changed dramatically with energies, which is consistent with the experiments.*

**PACS numbers:** 71.27.+a, 74.72.-h, 76.60.-k

**Key words:** incommensurate magnetic fluctuations,  $t$ - $J$  model, fermion-spin theory

It has become clear in the past several years that copper oxide materials are among the most complex systems studied in condensed matter physics and show many unusual magnetic properties.<sup>[1]</sup> The single common feature in copper oxide materials is the two-dimensional (2D) CuO<sub>2</sub> plane, while the unusual magnetic fluctuation is closely related to the fact that copper oxide materials are doped Mott insulators, obtained by chemically adding charge carriers to a strongly correlated antiferromagnetic (AF) insulating state,<sup>[2]</sup> therefore the magnetic properties of copper oxide materials mainly depend on the extent of dopings, and the regimes have been classified into the underdoped, optimally doped, and overdoped, respectively. The undoped copper oxide materials are insulating systems,<sup>[2]</sup> and well understood in terms of the 2D antiferromagnet with an AF long-range-order (AFLRO), then it is clearly of great interest to investigate the evolution of the magnetic correlation with charge carrier dopings. A series of inelastic neutron scattering, muon-spin-resonance, and nuclear magnetic resonance (NMR) measurements<sup>[3-5]</sup> show that when the commensurate AFLRO phase is suppressed and the doped hole concentration exceeds 5%, the incommensurate dynamical short-range magnetic correlations are developed, where the magnetic Bragg peak in the dynamical spin susceptibility broadens and develops a structure with four peaks located at the reciprocal space positions  $[(1 \pm \delta)\pi, \pi]$  and  $[\pi, (1 \pm \delta)\pi]$  (square lattice notations, unit lattice constant), while the incommensurability amplitude  $\delta(x)$

does not depend on energies. Even more remarkable is that  $\delta(x)$  is a universally increasing function of the hole concentration.<sup>[6]</sup> It is widely believed that the same correlation, that leads to the insulating AF state in copper oxide materials at small doping, also leads to the superconductivity in the underdoped and optimally doped regimes.<sup>[2]</sup>

The incommensurate magnetic correlation of copper oxide materials in the underdoped regime has been extensively studied theoretically within some strongly correlated models.<sup>[7]</sup> Based on the two-band model, it has been shown that the origin of the incommensurate spin phase is induced by the formation of the charged magnetic domain lines.<sup>[8]</sup> The analytical calculations and numerical simulations of the ground-state energy and magnetic susceptibility within the 2D Hubbard model show that at the zero temperature the commensurate AF state is unstable against domain-wall formation for arbitrary small deviations from the half-filling, and the resulting incommensurate antiferromagnet remains initially insulating.<sup>[9]</sup> It has been predicted that the development of an incommensurate spiral phase is doped away from the half-filling.<sup>[10]</sup> Moreover, many authors<sup>[11]</sup> use a simple 2D band-structure model incorporating the marginal Fermi-liquid self-energy corrections to calculate the spin fluctuation spectrum at low energies, and the results show that the features in the band-structure incorporating the marginal Fermi-liquid self-energy lead to peaks in the spin structure factor at the incommensurate wave vectors.

\*The project at Beijing Normal University supported by National Natural Science Foundation of China under Grant No. 10074007, and the Grant from Ministry of Education of China, the project at Tamkang University supported in part by the National Science Council under Grant No. NSC 87-2112-M-023-004

However, the exact origin of the incommensurability still is controversial. To shed light on this issue, we, in this paper, try to study the doping dependence of the magnetic fluctuations in the underdoped copper oxide materials within the fermion-spin theory. Our results show that in the underdoped regime, the magnetic Bragg peaks from the dynamical spin structure factor  $S(k, \omega)$  is incommensurate with the lattice. Although the incommensurability  $\delta(x)$  is almost energy-independent, the dynamical spin susceptibility  $\chi''(k, \omega)$  at the incommensurate wave vectors is changed dramatically with energies.

Among the microscopic models the most helpful for discussion of the physical properties of copper oxide materials is the  $t$ - $J$  model,<sup>[12]</sup>

$$H = -t \sum_{i\eta\sigma} C_{i\sigma}^\dagger C_{i+\eta\sigma} + \text{h.c.} - \mu \sum_{i\sigma} C_{i\sigma}^\dagger C_{i\sigma} + J \sum_{i\eta} \mathbf{S}_i \cdot \mathbf{S}_{i+\eta}, \quad (1)$$

supplemented by the on-site local constraint

$$\sum_{\sigma} C_{i\sigma}^\dagger C_{i\sigma} \leq 1$$

to avoid the double occupancy, where  $\hat{\eta} = \pm\hat{x}, \pm\hat{y}$ ,  $C_{i\sigma}^\dagger$  ( $C_{i\sigma}$ ) are the electron creation (annihilation) operators,  $\mathbf{S}_i = C_{i\sigma}^\dagger \boldsymbol{\sigma} C_{i\sigma} / 2$  are spin operators with  $\boldsymbol{\sigma} = (\sigma_x, \sigma_y, \sigma_z)$  as Pauli matrices, and  $\mu$  is the chemical potential. This  $t$ - $J$  model was originally introduced as an effective Hamiltonian of the large- $U$  Hubbard model,<sup>[12]</sup> where the on-site Coulomb repulsion  $U$  is very large as compared with the electron hopping energy  $t$ , which leads to that electrons become strongly correlated to avoid double occupancy, therefore the strong electron correlation in the  $t$ - $J$  model manifests itself by the electron single occupancy on-site local constraint. This is why the crucial requirement is to impose this electron on-site local constraint for a proper understanding of the physics of copper oxide materials.<sup>[13]</sup> This electron single occupancy on-site local constraint can be treated exactly in analytical calculations within the fermion-spin theory,<sup>[14]</sup>  $C_{i\uparrow} = h_i^\dagger S_i^-$ ,  $C_{i\downarrow} = h_i^\dagger S_i^+$ , where the spinless fermion operator  $h_i$  describes the charge (holon) degrees of freedom, while the pseudospin operator  $S_i$  describes the spin (spinon) degrees of freedom. Then the fermion-spin theory naturally incorporates the physics of the charge-spin separation. In this

fermion-spin representation, the low-energy behavior of the  $t$ - $J$  model (1) can be expressed as

$$H = t \sum_{i\eta} h_{i+\eta}^\dagger h_i (S_i^+ S_{i+\eta}^- + S_i^- S_{i+\eta}^+) + \mu \sum_i h_i^\dagger h_i + J_{\text{eff}} \sum_{i\eta} (\mathbf{S}_i \cdot \mathbf{S}_{i+\eta}) \quad (2)$$

with

$$J_{\text{eff}} = J[(1 - \delta)^2 - \phi^2],$$

the holon particle-hole parameter  $\phi = \langle h_i^\dagger h_{i+\eta} \rangle$ , and  $S_i^+$  and  $S_i^-$  are the pseudospin raising and lowering operators, respectively. As a consequence, the kinetic part in the  $t$ - $J$  model has been expressed as the holon-spinon interaction in the fermion-spin representation, which dominates the physics in the underdoped and optimally doped regimes in copper oxide materials.

Within the framework of the charge-spin separation, it has been shown<sup>[15]</sup> that the spin fluctuation couples only to spinons, while the strong correlation between holons and spinons can be considered through the holon's order parameters entering in the spinon propagator. In this case, the particularly universal behavior of the integrated spin structure factor and integrated spin susceptibility in the underdoped regime has been discussed<sup>[16]</sup> within the fermion-spin theory by considering spinon fluctuations around the mean-field solution, where the spinon part is treated by the loop expansion to the second order. Following their discussions,<sup>[16]</sup> we can obtain the dynamical spin structure factor and susceptibility as

$$\begin{aligned} \tilde{S}(k, \omega) &= \text{Re} \int_0^\infty dt e^{i\omega(t-t')} D(k, t-t') \\ &= 2[1 + n_H(\omega)] \text{Im} D(k, \omega), \end{aligned} \quad (3)$$

$$\begin{aligned} \chi''(k, \omega) &= (1 - e^{-\beta\omega}) S(k, \omega) \\ &= 2 \text{Im} D(k, \omega), \end{aligned} \quad (4)$$

respectively, where the full spinon Green's function is

$$D^{-1}(k, \omega) = D^{(0)-1}(k, \omega) - \Sigma_s^{(2)}(k, \omega)$$

with the mean-field spinon Green's function<sup>[17]</sup>

$$D^{(0)-1}(k, \omega) = \frac{\omega^2 - \omega_k^2}{B_k},$$

and the second-order spinon self-energy from the holon pair bubble is

$$\Sigma_s^{(2)}(k, \omega) = -\left(\frac{Zt}{N}\right)^2 \sum_{pp'} (\gamma_{p'+p+k} + \gamma_{k-p'})^2 \frac{B_{k+p}}{2\omega_{k+p}} \left( \frac{F_1(k, p, p')}{\omega + \xi_{p+p'} - \xi_{p'} + \omega_{k+p}} - \frac{F_2(k, p, p')}{\omega + \xi_{p+p'} - \xi_{p'} - \omega_{k+p}} \right), \quad (5)$$

where

$$\gamma_k = \frac{1}{Z} \sum_{\hat{\eta}} e^{ik \cdot \hat{\eta}},$$

$Z$  is the number of the nearest neighbor sites,

$$B_k = \Delta[2\chi_z(\epsilon\gamma_k - 1) + \chi(\gamma_k - \epsilon)],$$

$$\Delta = 2ZJ_{\text{eff}},$$

$$\epsilon = 1 + 2t\phi/J_{\text{eff}},$$

$$F_1(k, p, p') = n_F(\xi_{p+p'})[1 - n_F(\xi_{p'})] \\ + [1 + n_B(\omega_{k+p})][n_F(\xi_{p'}) - n_F(\xi_{p+p'})],$$

$$F_2(k, p, p') = n_F(\xi_{p+p'})[1 - n_F(\xi_{p'})] \\ - n_B(\omega_{k+p})[n_F(\xi_{p'}) - n_F(\xi_{p+p'})],$$

$n_F(\xi_k)$  and  $n_B(\omega_k)$  are the fermion and boson distribution functions, respectively, while the mean-field holon excitation spectrum is  $\xi_k = 2Zt\chi\gamma_k + \mu$ , and the mean-field spinon excitation spectrum is

$$\omega_k^2 = \Delta^2(A_1\gamma_k^2 + A_2\gamma_k + A_3)$$

with

$$A_1 = \alpha\epsilon(\chi/2 + \epsilon\chi_z),$$

$$A_2 = \epsilon\{(1-Z)\alpha(\epsilon\chi/2 + \chi_z)/Z \\ - \alpha(C_z + C/2) - (1-\alpha)/(2Z)\},$$

$$A_3 = \alpha(C_z + \epsilon^2 C/2) + (1-\alpha)(1+\epsilon^2)/(4Z) \\ - \alpha\epsilon(\chi/2 + \epsilon\chi_z)/Z,$$

and the spinon correlation functions are

$$\chi = \langle S_i^+ S_{i+\hat{\eta}}^- \rangle, \quad \chi_z = \langle S_i^z S_{i+\hat{\eta}}^z \rangle,$$

$$C = (1/Z^2) \sum_{\hat{\eta}\hat{\eta}'} \langle S_{i+\hat{\eta}}^+ S_{i+\hat{\eta}'}^- \rangle,$$

$$C_z = (1/Z^2) \sum_{\hat{\eta}\hat{\eta}'} \langle S_{i+\hat{\eta}}^z S_{i+\hat{\eta}'}^z \rangle.$$

In order not to violate the sum rule of the correlation function  $\langle S_i^+ S_i^- \rangle = 1/2$  in the case without AFLRO, the important decoupling parameter  $\alpha$  has been introduced in the mean-field calculation, which can be regarded as the vertex correction.<sup>[17]</sup> All the above mean-field order parameters  $\chi$ ,  $\chi_z$ ,  $C$ ,  $C_z$ ,  $\phi$ , the decoupling parameter  $\alpha$ , and chemical potential  $\mu$  have been determined by the self-consistent calculation.<sup>[17]</sup>

We have performed a numerical calculation for the dynamical spin structure factor  $S(k, \omega)$ , and the results of the  $S(k, \omega)$  spectrum along the line  $k = [1/2, k_y]$  (unit  $2\pi$ ) at the doping (a)  $x = 0$  and (b)  $x = 0.09$  with the temperature  $T = 0.01J$  and the energy  $\omega = 0.125J$  for the parameter  $t/J = 2.5$  are plotted in Fig. 1.

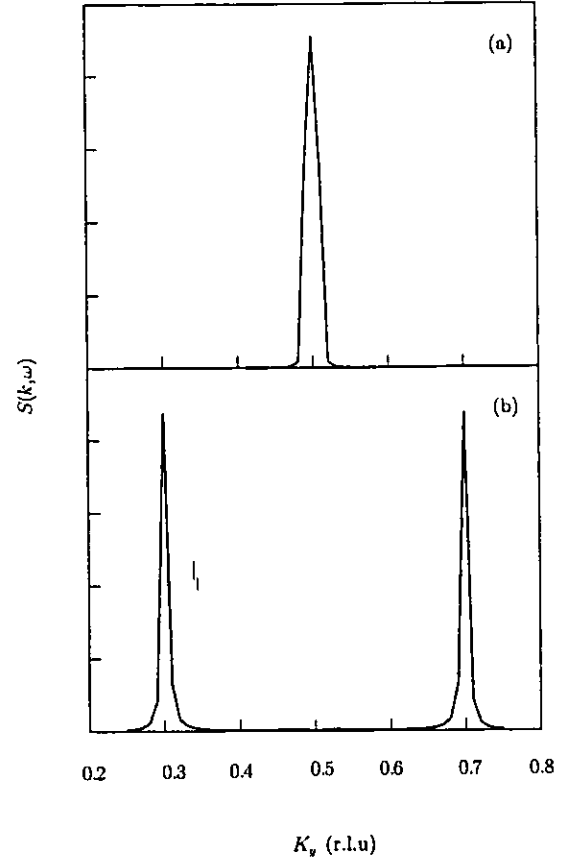


Fig. 1 The dynamical spin structure factor  $S(k, \omega)$  along the line  $k = [1/2, k_y]$  (unit  $2\pi$ ) at the doping (a)  $x = 0$  and (b)  $x = 0.09$  with the temperature  $T = 0.01J$  and the energy  $\omega = 0.125J$  for the parameter  $t/J = 2.5$ .

Our result shows that in the undoped regime, there is an AF commensurate peak at the AF wave vector position, while this commensurate peak is split into two peaks in the underdoped regime, the positions of these two split peaks are incommensurate with the lattice. Moreover, the present  $S(k, \omega)$  spectrum has been used to extract the doping dependence of the incommensurability  $\delta(x)$ , which is defined as the deviation of the peak position from AF wave vector position, and the result is shown in Fig. 2. The main characteristic of the doping dependence of the modulated spin correlation in Fig. 2 is that there is a nonlinear relation between the incommensurability  $\delta(x)$  and the hole concentration  $x$ , i.e., the incommensurability amplitude  $\delta(x)$  increases progressively with the hole concentration at the lower doped regime, but saturates at the higher doped regime. Our theoretical results are qualitatively consistent with the experimental observations from copper oxide materials, where the spin fluctuation scattering remains the commensurability at the AF wave vector position in the undoped regime,<sup>[3-6]</sup> and increasing

dopings, there is a commensurate-incommensurate transition in the spin fluctuation geometry, and the incommensurate scattering in the underdoped regime corresponds to four 2D rods at  $[(1 \pm \delta)\pi, \pi]$  and  $[\pi, (1 \pm \delta)\pi]$ . In Fig. 3, we plot the dynamical spin structure factor  $S(k, \omega)$  at the doping  $x = 0.06$  for the parameter  $t/J = 2.5$  and temperature  $T = 0.01J$  with the energy  $\omega = 0.05J$  (solid line),  $\omega = 0.125J$  (dashed line),  $\omega = 0.25J$  (dotted line), and  $\omega = 0.5J$  (dashed-dotted line), where we find that although the position of the incommensurate peaks is almost energy-independent, the incommensurate peaks are broadened and suppressed with increasing energies, which leads to that the lifetime of the excitation decreases quickly with increasing energies. These results are also consistent with the experiments.<sup>[3-6]</sup>

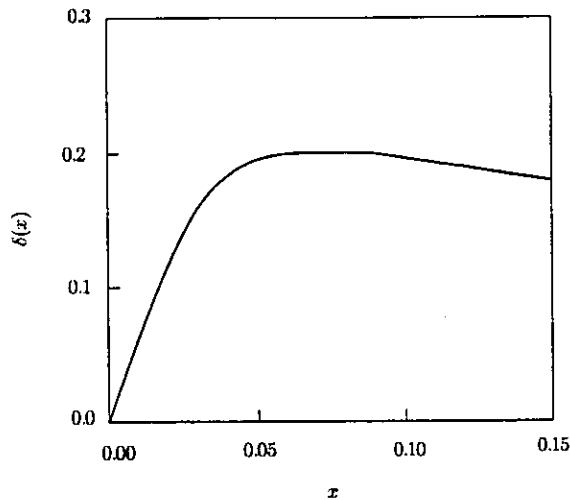


Fig. 2 The doping dependence of the incommensurability  $\delta$  of the magnetic fluctuation.

In correspondence with the  $S(k, \omega)$  spectrum, the numerical results of the dynamical spin susceptibility  $\chi''(Q', \omega)$  at the doping  $x = 0.06$  for the parameter  $t/J = 2.5$  and energy  $\omega = 0.125J$  with the temperature  $T = 0.1J$  (solid line),  $T = 0.2J$  (dashed line),  $T = 0.4J$  (dotted line) and  $T = 0.6J$  (dashed-dotted line) are plotted in Fig. 4, where the incommensurate wave vector  $Q' = [1/2, (1 - \delta)/2]$  (unit  $2\pi$ ) with  $\delta = 0.2$ . This result shows that in the underdoped regime, the low- and high-energy fluctuations coexist in the  $\chi''(Q', \omega)$  spectrum, the excitations are remarkably sharp at low energies ( $\omega < J$ ). Moreover, the low-energy peak is temperature-dependent, and suppressed with increasing temperatures, while the high-energy peak is almost temperature-independent, which are qualitatively consistent with the experiments.<sup>[3-6]</sup> The low-energy peak in the  $\chi''(Q', \omega)$  spectrum is due to the

AF fluctuation, which will exist even in the undoped case and dominate the neutron-scattering and NMR processes, while the high-energy peak may be due to the contribution of the free-fermion-like component of the systems, which induces to a large extent the main effect of the static spin correlations.

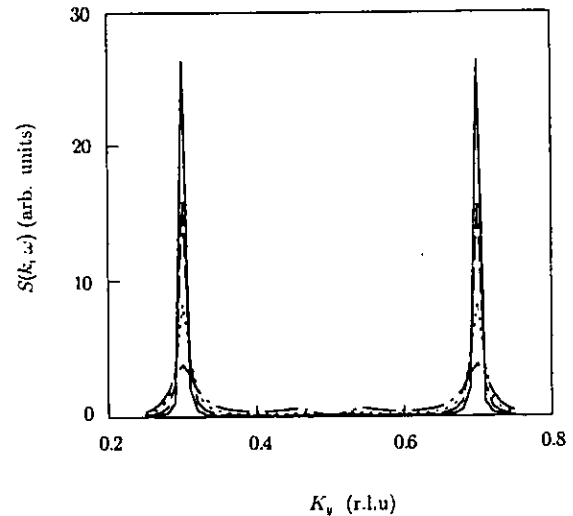


Fig. 3 The dynamical spin structure factor  $S(k, \omega)$  along the line  $k = [1/2, k_y]$  (unit  $2\pi$ ) at the doping  $x = 0.06$  for the parameter  $t/J = 2.5$  and temperature  $T = 0.01J$  with the energy  $\omega = 0.05J$  (solid line),  $\omega = 0.125J$  (dashed line),  $\omega = 0.25J$  (dotted line) and  $\omega = 0.5J$  (dashed-dotted line).

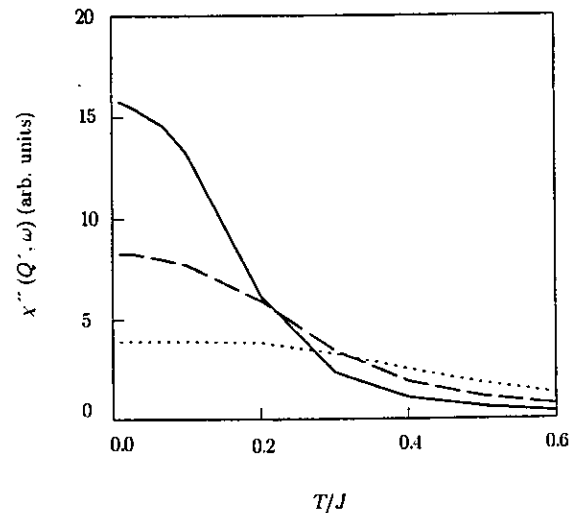


Fig. 4 The dynamical spin susceptibility  $\chi''(Q', \omega)$  at the doping  $x = 0.06$  for the parameter  $t/J = 2.5$  with the energy  $\omega = 0.125J$  (solid line),  $\omega = 0.25J$  (dashed line) and  $\omega = 0.6J$  (dotted line), where the incommensurate wave vector  $Q' = [1/2, (1 - \delta)/2]$  (unit  $2\pi$ ) with  $\delta = 0.2$ .

Our results indicate that as a function of dopings the  $t$ - $J$  model has a tendency to develop incommensurate cor-

relations between the spins. At the half-filling, there are no charge degrees of freedom, and the spinons are primarily localized on the lattice sites. With increasing dopings, a mobile holon produces a "roton"-like distortion of the spinon background. In this case, the spinon moves self-consistently in the background of holons, and the cloud of distorted holon background is to follow spinons, therefore the mechanism of the incommensurate type of structure in copper oxide materials away from the half-filling is most likely related to the holon motion. This is why the position of the incommensurate peaks can be determined in the present study by the  $t$ - $J$  model, while the spinon energy dependence is ascribed purely to self-energy effects which arise from the holon-spinon interaction.

In summary, we have discussed the doping dependence

of the magnetic fluctuation of copper oxide materials in the underdoped regime within the  $t$ - $J$  model. Our results show that away from the half-filling, the magnetic Bragg peaks from the dynamical spin structure factor spectrum  $S(k, \omega)$  are incommensurate with the lattice. Although the incommensurability  $\delta(x)$  is almost energy-independent, the dynamical spin susceptibility  $\chi''(Q', \omega)$  at the incommensurate wave vectors is changed dramatically with energies. Our theoretical results are qualitatively consistent with the experiments.

### Acknowledgments

The authors would like to thank Profs Z.B. Su, T. Xi-ang and L. Yu for helpful discussions.

### References

- [1] See, e.g., *High Temperature Superconductivity*, Proc. Los Alamos Symp., 1989, eds K.S. Bedell, D. Coffey, D.E. Meltzer, D. Pines and J.R. Schrieffer, Addison-Wesley, Redwood City, California (1990).
- [2] M.A. Kastner, R.J. Birgeneau, G. Shirane and Y. Endoh, *Rev. Mod. Phys.* **70** (1998) 897; A.P. Kampf, *Phys. Rep.* **249** (1994) 219.
- [3] S.W. Cheong, G. Aeppli, T.M. Mason, H. Mook, S.M. Hayden, P.C. Canfield, Z. Fisk, K.N. Clausen and J.L. Martinez, *Phys. Rev. Lett.* **67** (1991) 1791; T.E. Mason, G. Aeppli, S.M. Hayden, A.P. Ramirez and H.A. Mook, *Phys. Rev. Lett.* **71** (1993) 919; K. Yamada, S. Wakimoto, G. Shirane, C.H. Lee, M.A. Kastner, S. Hosoya, M. Greven, Y. Endoh and R.J. Birgeneau, *Phys. Rev. Lett.* **75** (1995) 1626.
- [4] T.M. Thurston, P.M. Gehring, G. Shirane, R.J. Birgeneau, M.A. Kastner, Y. Endoh, M. Matsuda, K. Yamada, H. Kojima and I. Tanaka, *Phys. Rev.* **B46** (1992) 9128; G. Shirane, R.J. Birgeneau, Y. Endoh, P. Gehring, M.A. Kastner, K. Kitazawa, H. Kojima, I. Tanaka, T.R. Thurston and K. Yamada, *Phys. Rev. Lett.* **63** (1989) 330; R.J. Birgeneau, D.R. Gabbe, H.P. Jentsen, M.A. Kastner, P.J. Picone, T.R. Thurston, G. Shirane, Y. Endoh, M. Sato, K. Yamada, Y. Hidaka, M. Oda, Y. Enomoto, M. Suzuki and T. Murakami, *Phys. Rev.* **B38** (1988) 6614.
- [5] M. Matsuda, K. Yamada, Y. Endoh, T.R. Thurston, G. Shirane, R.J. Birgeneau, M.A. Kastner, I. Tanaka and H. Kojima, *Phys. Rev.* **B49** (1994) 6958; T.R. Thurston, R.J. Birgeneau, M.A. Kastner, N.W. Preyer, G. Shirane, Y. Fujii, K. Yamada, Y. Endoh, K. Kakurai, M. Matsuda, Y. Hidaka and T. Murakami, *Phys. Rev.* **B40** (1989) 4585; S. Wakimoto, G. Shirane, Y. Endoh, K. Hirota, S. Ueki, K. Yamada, R.J. Birgeneau, M.A. Kastner, Y.S. Lee, P.M. Gehring and S.H. Lee, *Phys. Rev.* **B60** (1999) R769.
- [6] Y. Fukuzumi, K. Mizuhashi, K. Takenaka and S. Uchida, *Phys. Rev. Lett.* **76** (1996) 684; K. Yamada, C.H. Lee, K. Kurahashi, J. Wada, S. Wakimoto, S. Ueki, H. Kimura, Y. Endoh, S. Hosoya, G. Shirane, R.J. Birgeneau, M. Greven, M.A. Kastner and Y.J. Kim, *Phys. Rev.* **B57** (1998) 6165.
- [7] S.A. Kivelson, E. Fradkin and V.J. Emery, *Nature* **393** (1998) 550; F. Marcini, D. Villani and H. Matsumoto, *Phys. Rev.* **B57** (1998) 6145; D. Poilblanc and T.M. Rice, *Phys. Rev.* **B39** (1989) 9749; Q. Si, Y. Zha, K. Levin and J.P. Lu, *Phys. Rev.* **B47** (1993) 9055; R.J. Gooding, K.J.E. Vos and P.W. Leung, *Phys. Rev.* **B49** (1994) 4119; A. Moreo, E. Dagotto, T. Jolicoeur and J. Riera, *Phys. Rev.* **B42** (1990) 6283.
- [8] J. Zannen and O. Gunnarsson, *Phys. Rev.* **B40** (1989) 7391.
- [9] H.J. Schulz, *Phys. Rev. Lett.* **64** (1990) 1445; T. Giamarchi and C. Lhuillier, *Phys. Rev.* **B42** (1990) 10641.
- [10] B.I. Shraiman and E.D. Siggia, *Phys. Rev. Lett.* **62** (1989) 1564.
- [11] P.B. Littlewood, J. Zannen, G. Aeppli and H. Monien, *Phys. Rev.* **B48** (1993) 487.
- [12] P.W. Anderson, *Science* **235** (1987) 1196; F.C. Zhang and T.M. Rice, *Phys. Rev.* **B37** (1988) 3759.
- [13] L. Zhang, J.K. Jain and V.J. Emery, *Phys. Rev.* **47** (1993) 3368; S.P. Feng, J.B. Wu, Z.B. Su and L. Yu, *Phys. Rev.* **B47** (1993) 15192.
- [14] S.P. Feng, Z.B. Su and L. Yu, *Phys. Rev.* **B49** (1994) 2368; *Mod. Phys. Lett.* **B7** (1993) 1013.
- [15] L.B. Ioffe and A.I. Larkin, *Phys. Rev.* **B39** (1989) 8988.
- [16] Shiping Feng and Zhongbing Huang, *Phys. Rev.* **B57** (1998) 10328.
- [17] Shiping Feng and Yun Song, *Phys. Rev.* **B55** (1997) 642.